Addition Coupled Electron Transfer (ACET) and Addition Coupled Proton Coupled Electron Transfer (ACPCET)

Yumiao Ma*[a,b] and Aqeel A. Hussein*[c]

[a] Mr Yumiao Ma
Institution BSJ Institute, Haidian, Beijing, 100084, People's Republic of China. ymma@bsj-institute.top
[b] Hangzhou Yanqu Information Technology Co., Ltd. Xihu District, Hangzhou City, Zhejiang Province, 310003, People's Republic of China
[c] Dr. Aqeel Hussein
Department of Pharmacy, College of Medicine, Komar University of Science and Technology, Sulaymaniyah, Kurdistan Region, Iraq; Email: aqeel.alaa@komar.edu.iq
Supporting information for this article is given via a link at the end of the document.

Abstract: The new types of elementary reaction in which a nucleophilic addition (A) to quinones is coupled with electron transfer (ET) and even further proton transfer (PT) are suggested herein by density functional theory calculation, which are called Addition Coupled Electron Transfer (ACET) and Addition Coupled Proton Coupled Electron Transfer (ACPCET). With a [2.2]paracyclophane-derived biquinone as the substrate, the nature of nucleophilic addition onto its sp2 carbons exhibits a change from stepwise A-ET-PT to ACET-PT and further to ACPCET, in parallel with the decreased nucleophilicity of the attacking reagent. In addition, we further proposed six possible potential energy surfaces and the coupling modes among A, ET and PT, among which three have been found in this work. Quasi-classical trajectory shows that the ACET and PT event can also be dynamically concerted even for an ACET-PT mechanism.

Introduction

Since its first being proposed in 1981[1], the proton-coupled electron transfer (PCET) has become a well-known concept, and both its theory[2] and practical use[3] have been continuously explored. Under this scheme, besides the Hydrogen Atom Transfer (HAT) reaction, in which both the proton and electron being transferred involves the same orbital, during the reaction of a hydrogen donor (AH) and an acceptor (B) to give A and BH, there are three possible modes. These modes are (1) stepwise electron transfer (ET) to form $AH^{+\bullet}$ and $B^{-\bullet}$ followed by a proton transfer (PT), (2) stepwise PT affording A^- and BH^+ followed by an ET, and (3) a concerted proton-electron transfer in one elementary step called PCET, especially when single PT or ET is thermodynamically unfavorable (Figure 1a-i). The key point of PCET is that PT and ET can interplay and promote each other: ET leads to increased acidity of the A–H bond, promoting the PT process; at the meantime the negative charge resulted by PT on A further promotes ET. The inter-promoting nature of PT and ET enables their coupling, causing the elementary step of PCET as a result, and PCET has been proven to be a useful tool to activate the hydrogen transfer. Overall, the PCET has been shown to have many synthetic applications through either oxidative or reductive manners (Figure 1a-ii) due to the kinetic advantages gained in the mechanistic pathway (Figure 1a-iii). [3b]

The potential reaction mode to couple with ET is not limited to PT. We suggest in this work that the coupling of a nucleophilic addition with ET or even PCET is also possible, resulting in new type of elementary reaction that has not been explored. In this regard, the nucleophilic addition reaction towards an olefin substrate is, to some extent, similar to PT from an acidic substrate: they both create a partial negative charge which is prone to be oxidized, and both are activated by a more oxidized (electrophilic) substrate. As a result, the addition reaction is possible to be coupled to, and be promoted by an ET event. If this elementary step does exist, it will open a door to new methodologies for the activation of weak nucleophiles by introduction of ET, just like the case for PCET.

To set up our new elementary reaction, we have selected [2.2]paracyclophane-derived biquinone compound **1** (Figure 1b) as the model substrate, and compared the mechanism in the presence of nucleophiles with various nucleophilicity. As shown in Figure 1b, the addition of various nucleophiles based on their strength will lead to different modes of reactions as indicated in our results. Therefore, here we report the first example of nucleophilic addition coupled with PT and ET, leading to the new elementary reaction called Addition-Coupled Electron Transfer (ACET) and Addition-Coupled Proton-Coupled Electron Transfer (ACPCET)[4]. In order to establish the mechanism of ACET and ACPCET, three questions among this study will be raised concerning the nature of the process such as (i) what is the possibility of open-shelled intermediates during the addition pathway? (ii) do the process of A, PT, and ET occur in a stepwise or concerted manner? and (iii) is the whole process dynamically stepwise or concerted from a molecular dynamic's perception when quasiclassical molecular dynamic (QCMD) simulations are performed? All of the study is conducted using both density functional theory (DFT) and multireference method calculations.

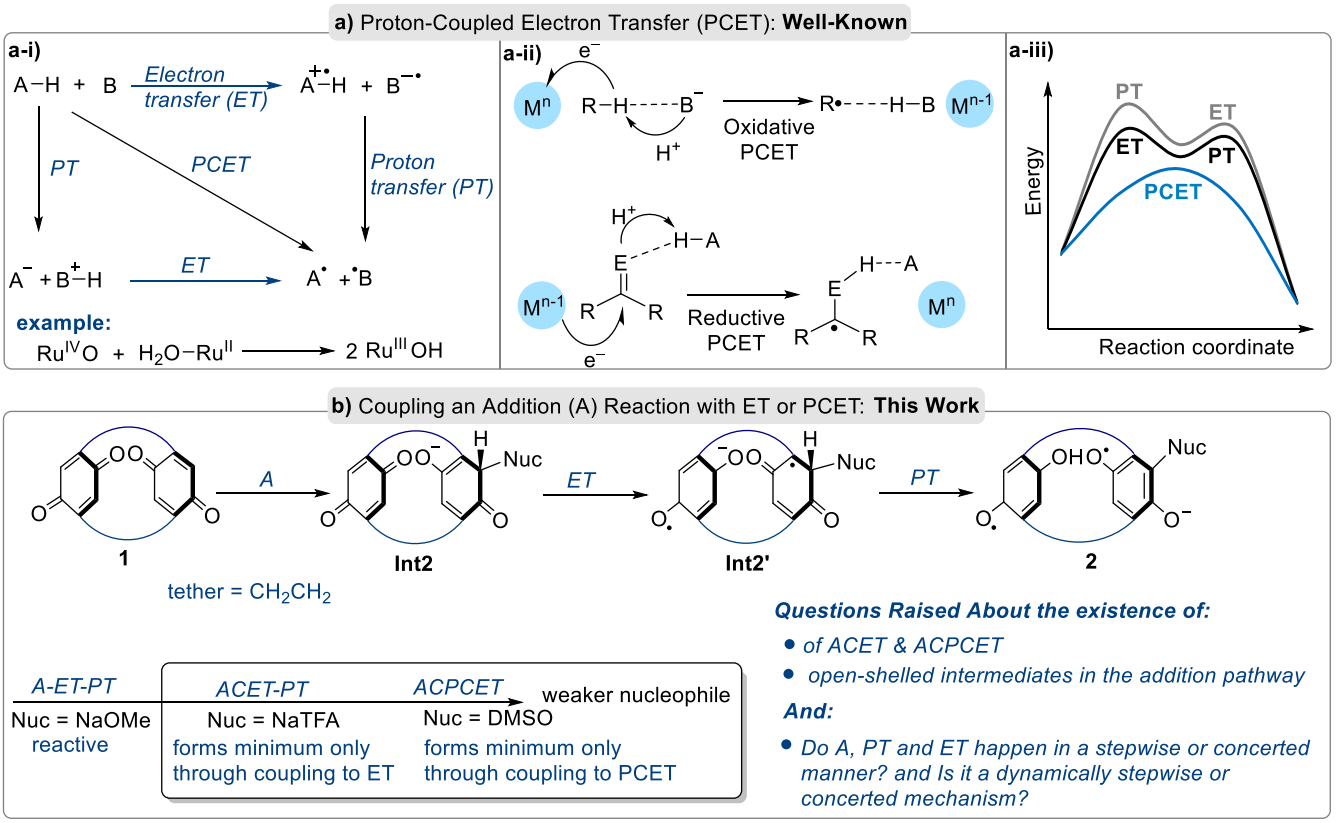

Figure 1. (a-i) The general concept of PCET, (a-ii) the oxidative and reductive PCET, and (a-iii) the kinetic advantage of PCET. (b) Nucleophilic addition to electron-deficient olefins with questions raised about the new concept of ACET and ACPCET.

Computational Methods

The Gaussian 16 package [5] was employed to perform all the calculations, with the Gaussian 09 default integral grid. The ωB97X-D functional[6] was used for all calculations. For geometry optimization, the def2-SVP [7] basis set was employed. Frequency calculations were followed to ensure stationary points were found, and to obtain Gibbs free energy correction at room temperature. Single point calculations were performed with the def2-TZVPP basis set. Both geometry optimization and single point calculations were performed under SMD implicit solvation using tetrahydrofuran (THF) as the medium solvent.[8] The stability of wavefunction was checked for all the structures in this study. The spin density analysis were performed with the Multiwfn program.[9] The molecular geometry and isosurface were plotted with CYLView [10] and VMD.[11] The quasiclassical trajectory molecular dynamics simulations were performed using the PROGDYN program.[12] The initial geometry for each trajectory was generated by adding displacements that follows a QM-like Gaussian distribution to all vibrational modes higher than 10 cm^{-1} of **TS2**. Each real normal mode was given its zero-point energy plus a random Boltzmann sampling of the thermal energy available at 298.15 K. Trajectories were propagated at the SMD(THF)-ωB97X-D/def2-SVP level of theory in both the forward and backward directions, until the product formed, or the length of trajectory is longer than 300 fs. The multireference calculations, complete active space self-consistent field (CASSCF) and N-electron Valence State Perturbation Theory (NEVPT2),[13] were performed using the ORCA program,[14] with the natural orbital derived from the triplet state UHF calculations as the reference. The crossing point between the close-shelled singlet (CSS) and open-shelled singlet (OSS) potential energy surface (PES) was located by the self-written open-source KST48 program.[15]

Results and Discussion

Initial Insight. Compound **1** has been synthesized and characterized by Staab by oxidizing its phenol precursor in 1973.[16] It was chosen as the model substrate in this work, because it bears two quinone rings connected by two short and rigid $(CH_2)_2$ linkers, enabling short contact of the two reactive rings. As a result, it is of concern that once a nucleophile attacks one quinone ring, leading to an enolate (**Int2** in Figure 1b) whether the other quinone ring could act as an intramolecular oxidant to achieve an open-shelled compound **Int2'**. Furthermore, the delicate structure of **1** enables an intramolecular PT from **Int2'** across the two quinone rings, affording the final biradical product **2**. Of interests in this paper is whether these A, PT, and ET processes can efficiently couple, both in terms of minimum energy reaction path (MEP) and reaction dynamics.

Our first concern is whether the intermediates mentioned in Figure 1b can exist or not. The answer to this question depends on the nucleophilicity of the attacking reagent. So, we have selected here two nucleophiles, namely azide ion (N_3^-) and dimethyl sulfoxide (DMSO). Two typical two-dimensional potential energy surfaces along the reaction coordinate of both addition and hydrogen transfer are shown in Figure 2. On one hand, for a common nucleophile with enough nucleophilicity, the approaching to **1** leads to a minimum, corresponding to either close-shelled **Int2** or open-shelled **Int2'**. In this case, we expect that a stepwise A-ET-PT or A-PCET or ACET-PT should happen (Figure 2: top). On the other hand, when the nucleophilicity is extremely low, like the case with DMSO as the nucleophile, **Int2** and **Int2'** are unable to be a minimum on the potential energy surface (Figure 2: bottom). Thus, since **1** is thermodynamically unable to oxidize the nucleophile to initialize an ET-A-PT process (see Supporting Information for the redox

thermodynamics), the subsequent A, ET, and PT steps have to be coupled in one single elementary step corresponded to the ACPCET mechanism.

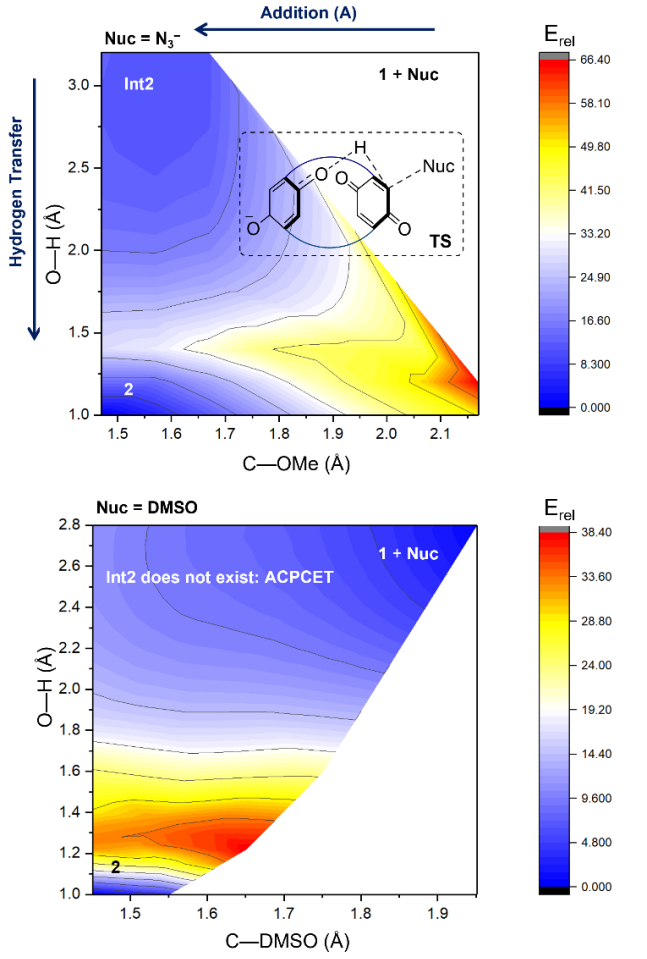

Figure 2. The two-dimensional potential energy contours for the overall A-ET-PT reaction, with N_3^- (top: when addition product is close-shelled means A-ET-PT or A-PCET whereas when addition product is open-shelled means ACET-PT which is ether dynamically stepwise or concerted) and DMSO (bottom) as the nucleophiles, respectively. Energies are shown in kcal/mol, and the interested bonds are labelled in the inner figure.

In the following parts, we separately discuss the three cases using three different nucleophiles are NaOMe, NaTFA, and DMSO, showing stepwise A-ET-PT, ACET-PT, or ACPCET.

Case I: Stepwise A-ET-PT (Nuc = NaOMe). With NaOMe as nucleophile, all the intermediates and transition states in Figure 1b can be located, as shown in Figure 3a. The complex of **1** with NaOMe, namely $\mathbf{1}_{\mathbf{NaOMe}}$, undergoes a rapid nucleophilic addition with a barrier of 4.7 kcal/mol, affording a close-shelled enolate $\mathbf{Int2}_{\mathbf{NaOMe}}$. Then, some geometry adjustment occurs, resulting in another minimum on the open-shelled potential energy surface, namely $\mathbf{Int2'}_{\mathbf{NaOMe}}$. The spin density isosurface shows that an intramolecular ET has happened in $\mathbf{Int2'}_{\mathbf{NaOMe}}$, in which the spin density on the quinone ring being attacked localizes on the *ortho*-site of the carbon attacked by the nucleophile, and the conjugating carbonyl group only shares little spin (Figure 3c). The spin density on the ring that is acting as the oxidant is delocalized over the two carbonyl groups. After the formation of $\mathbf{Int2'}_{\mathbf{NaOMe}}$, an intramolecular PT occurs through $\mathbf{TS2}_{\mathbf{NaOMe}}$ with a barrier of 17.0 kcal/mol. The evolution of the C–H bond being broken and O–H bond being formed along the Intrinsic Reaction Coordinate (IRC) of $\mathbf{TS2}_{\mathbf{NaOMe}}$ is shown in Figure 3b. The O–H bond slowly decreases to ~1.5 angstrom in the pre-TS region (up to IRC step ~-5) and is sharply shortened to ~1.0 angstrom through $\mathbf{TS2}_{\mathbf{NaOMe}}$. The change of C–H bond length is asynchronous with the O–H bond as it almost keeps unchanged at the pre-TS region, where it undergoes the first increase from IRC step -5 to 10 and then another increase starting from IRC step 10. The two increases correspond to two phases of the overall reaction: the PT phase from IRC point -60 to 10, and then the hydroxyl rotation phase which can be seen by comparing the geometry of step 10 (Figure 3b) and $\mathbf{2}_{\mathbf{NaOMe}}$ (Figure 3c). As for the spin density, all the points along the IRC are open-shelled, indicating that the reaction is almost a PT, although spin density at the *ortho*-carbon of both $\mathbf{Int2'}_{\mathbf{NaOMe}}$ and $\mathbf{TS2}_{\mathbf{NaOMe}}$ is delocalized onto the two oxygen atoms in the final product $\mathbf{2}_{\mathbf{NaOMe}}$ at the end of the reaction. According to the observations above, the presence of both $\mathbf{Int2}_{\mathbf{NaOMe}}$ and $\mathbf{Int2'}_{\mathbf{NaOMe}}$, the nature of in $\mathbf{TS2}_{\mathbf{NaOMe}}$, and the presence of ET in $\mathbf{Int2'}_{\mathbf{NaOMe}}$, we concluded that the overall reaction follows a stepwise A-ET-PT mechanism when NaOMe acts as a nucleophile.

Case II: ACET-PT (Nuc = NaTFA). We next used NaTFA as the nucleophile and a tetrahedral intermediate-like compound $\mathbf{Int2'}_{\mathbf{NaTFA}}$ was also located as the case for NaOMe, although it is much higher in energy as it is 44.3 kcal/mol above the complex formed by **1** and NaTFA, namely $\mathbf{1}_{\mathbf{NaTFA}}$. The ET-product $\mathbf{Int2'}_{\mathbf{NaTFA}}$ undergoes a PT through $\mathbf{TS2}_{\mathbf{NaTFA}}$ with an overall barrier of 57.8 kcal/mol to give the final product $\mathbf{2}_{\mathbf{NaTFA}}$. Although the barrier is rather high and causing the reaction experimentally inaccessible, it is still theoretically valuable in providing mechanistic insights into the elementary reaction modes. Notably, there is no minimum corresponding to the addition product with 2,6-dimethyl-1,4-benzoquinone as the substrate, indicating that the ET resulted by the second benzoquinone ring is essential. It is the ET event that stabilizes the addition product, causing $\mathbf{Int2'}_{\mathbf{NaTFA}}$ to be able to be a minimum. Although in this case the energetics of intermediates are high, it suggests the potential opportunity of using an ET event to promote addition reaction of weak nucleophiles in the future.

Although the formation of $\mathbf{Int2'}_{\mathbf{NaTFA}}$ and the following PT are similar to the NaOMe case, there is one substantial difference: in the NaTFA case the close-shelled singlet (CSS) **Int2** is no longer a minimum. By scanning the C–Nuc distance (see Supporting Information), the energy monotonously increases while NaTFA approaches on the CSS potential energy surface (PES). Instead, the addition product $\mathbf{Int2'}_{\mathbf{NaTFA}}$ can only exist on the open-shelled singlet (OSS) PES. On one hand, no transition state for the addition step was able to be found on both CSS and OSS PES. On the other hand, the crossing point between the CSS and OSS PES, **CP1**, at which the energy of the CSS and OSS state is degenerated, could be determined to be the critical point for the hopping from the CSS to the OSS PES. The downhill pathway starting from **CP1**, which is generated in a similar way to the Intrinsic Reaction Coordinate (IRC) and represents the reaction pathway across **CP1**, clearly shows that **CP1** connects directly to $\mathbf{1}_{\mathbf{NaTFA}}$ and $\mathbf{Int2'}_{\mathbf{NaTFA}}$ on the CSS and OSS PES, respectively. As a result, it can be inferred that the addition step proceeds through **CP1** instead of a transition state; once $\mathbf{1}_{\mathbf{NaTFA}}$ goes across **CP1**, it will hop into the OSS-PES, and falls down the downhill pathway to afford $\mathbf{Int2'}_{\mathbf{NaTFA}}$. In this case, the addition and ET are coupled in one elementary step (ACET). The difference between ACET and stepwise ET-A-PT will be further discussed in the later section.

In addition to the DFT calculation, the multi-reference calculations CASSCF and NEVPT2 [13] were also performed based on an active space with 12 orbitals and 12 electrons. The relative energy (shown in parentheses in Figure 4a) derived from NEVPT2 single point calculations were very close to the DFT results, supporting the reliability of the DFT results. According to the CASSCF-results, the electronic structure of the OSS state of **CP1** is almost contributed by the HOMO-LUMO excitation of ~97%. According to the CASSCF Optimized frontier orbitals (Figure 4c), the HOMO and LUMO distributes on the *ortho*-carbon atom to the NaTFA attacked site and the quinone ring

acting as the oxidant, respectively, which clearly reveals the existence of intramolecular single electron transfer.

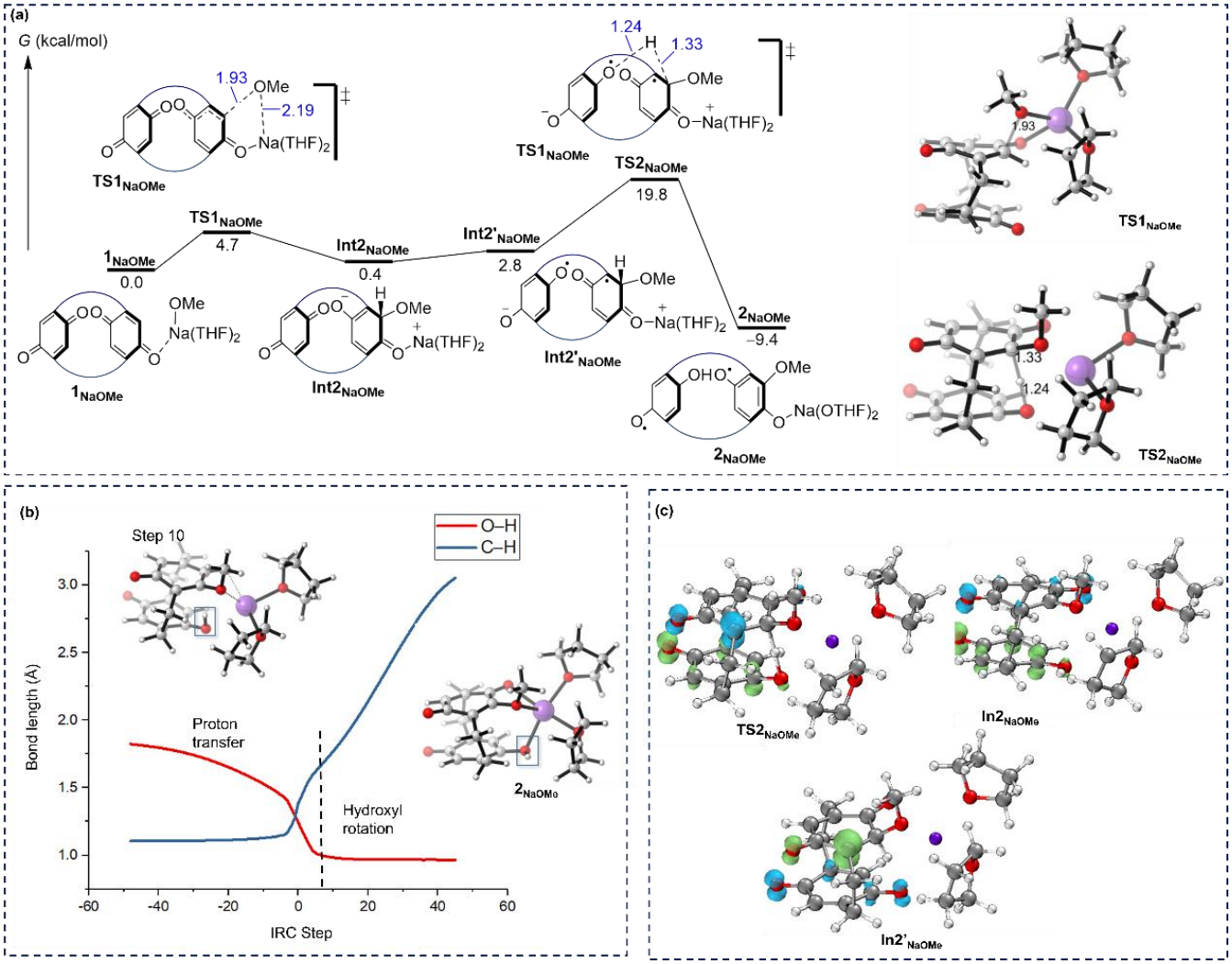

Figure 3. (a) The Gibbs free energy profile for the A-ET-PT reaction with NaOMe as the nucleophile. Distances are in Å. (b) the evolution of energy and key bond lengths along the IRC of **TS2$_{NaOMe}$**. (c) The spin density isosurface of the key species. Two explicit solvent molecules of THF were added to NaOMe during all steps.

Case III: ACPCET (Nuc = DMSO). We further moved to a weaker nucleophile DMSO compared with NaTFA. The extremely low nucleophilicity of DMSO is reflected by its higher addition barrier of 69.8 kcal/mol via **TS2$_{DMSO}$** (Figure 5a) and absence of both **Int2** and **Int2'** (see Figure 2-bottom) when compared to NaTFA (Figure 4). Thus, the overall A-PT-ET process proceeds through only one transition state **TS2$_{DMSO}$**. The IRC profile of **TS2$_{DMSO}$** can be divided into three stages (Figure 5b). First, the approaching of DMSO to the substrate carbon atom is accompanied by ET and the ACET phase appears up to the IRC step -10. Second, the PT phase appears from the IRC step 10 to ~30). Third, the hydroxyl rotation phase appears after the IRC step 30. Furthermore, we have plotted the eigenvalue of the total spin operator (*S***2) along the IRC pathway (Figure 5c). The complex remains close-shelled at the beginning of the addition phase due to the *S***2 is zero, however at the IRC step ~-30 the ET event suddenly occurs, giving a *S***2 of ~0.8. Then, the nucleophile continues approaching the substrate, although with a less slope, until it reaches ~step -10, where the PT process starts according to the decreasing O–H distance. Notably, although they are divided into different phases in order to magnify the asynchronousity of PT with ACET, the C–Nuc distance keeps decreasing after a short platform period in the PT phase, and finally reaches 1.40 Å in **2$_{DMSO}$**. The evolution of spin density along IRC shares a similar mode with the stepwise mechanism. Here, a close-shelled structure is initiated and followed by the ET event, while subsequently the *ortho*-carbon to the carbon being attacked accumulates spin density and finally the spin is delocalized onto all the carbonyl groups in **2$_{DMSO}$**.

To Distinguish the Mechanisms. Up to now, we have discussed three examples with different coupling modes among A, ET, PT. In order to further clarify their relationship, the schematic models of their potential energy surfaces are plotted in Figure 6. Considering the crossing between the close-shelled and open-shelled PESs, and in the presence of a strong nucleophile, the addition product **Int2** can be a minimum on the CSS PES. In this regard, if the crossing point occurs later than its formation, and the resulted ET product, namely open-shelled addition product **Int2'** is also a minimum, then the reaction goes through two transition states divided by one crossing point, affording a typical stepwise A-ET-PT process (Figure 6a). If the ET product **Int2'** is not a minimum, and directly leads to the product **2**, then the reaction follows an A-PCET mechanism (Figure 6b). On the other hand, if the crossing point appears earlier than the formation of **Int2**, an ET event should happen at the post-TS region of addition, and directly connects with the ACET product (Class II ACET, Figure 6d).

Furthermore, if the nucleophile is too weak to form a close-shelled

addition product **Int2** as a minimum, then we see the cases of Figure 6a, 6c and 6f. The difference between ET-A-PT and Class I ACET-PT relies on whether the "pure" ET product (namely $\mathbf{1}^-$ and Nuc^+ derived from the reaction Nuc + **1** → $\mathbf{1}^-$ +Nuc^+) is able to exist as a minimum on the open-shelled surface. If a minimum is formed, then a barrier has to be overcome for addition, and a stepwise ET-A-PT reaction occurs (Figure 6e). However, in the NaTFA case, there is no such ET product (see Table SI1 for the redox potential), and thus no addition TS on the open-shelled surface. Instead, after the ET event through the crossing point, the addition product with electron transferred is directly obtained, which is classified as the Class I ACET (Figure 6c). If even the ACET product **Int2'** cannot exist as a minimum, as seen for the DMSO case, only one transition state appears along the whole reaction, and gives a fully coupled ACPCET reaction (Figure 6f).

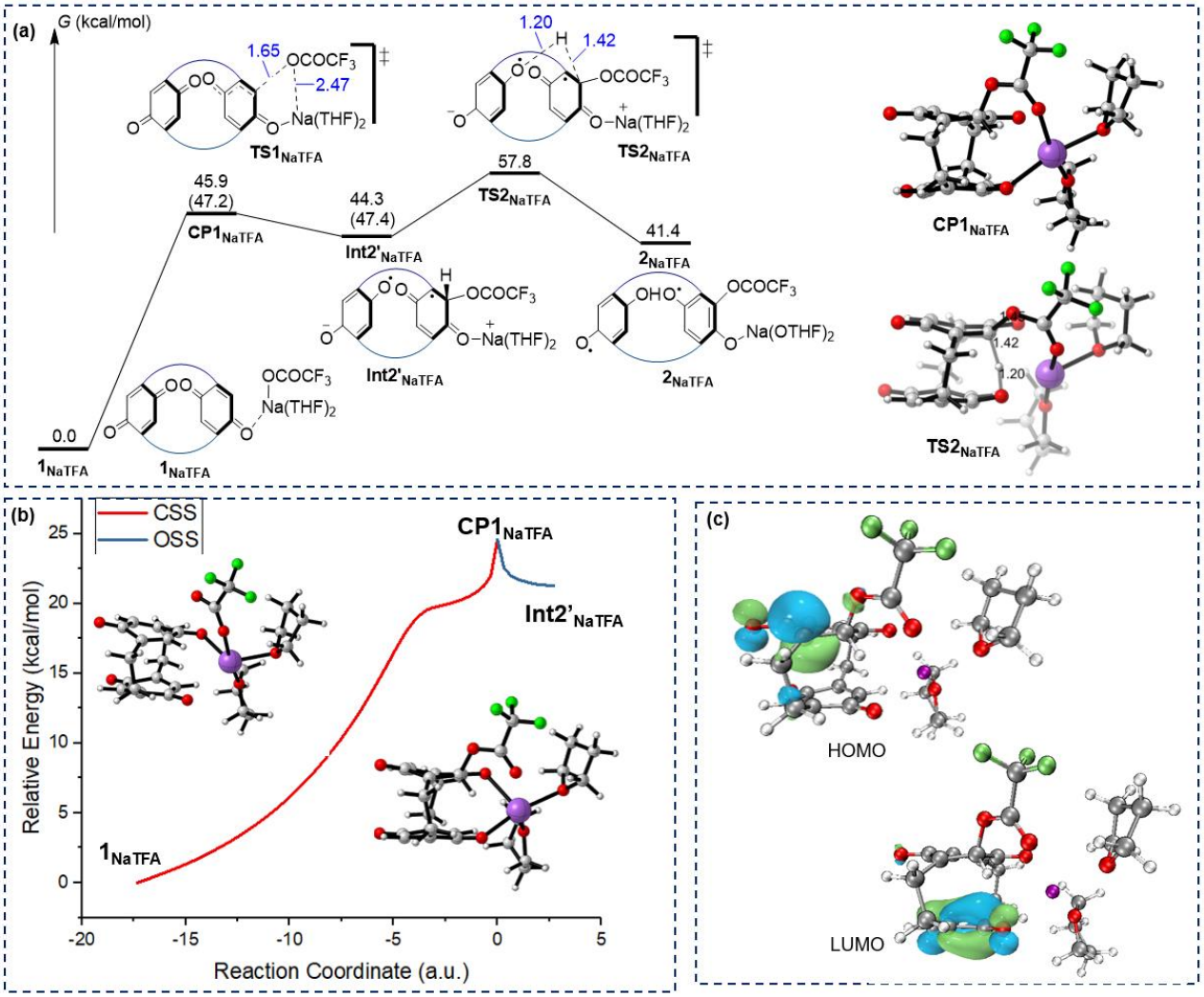

Figure 4. (a) The Gibbs free energy profile for the ACET-PT reaction with $Na(THF)_2(OCOCF_3)$ (noted as NaTFA) as the nucleophile. The relative free energies at NEVPT2(12,12) level are shown in parentheses. The geometries of the key species are shown, and distances are labelled in angstrom. (b) The downhill pathway starting from $\mathbf{CP1}_{\mathbf{NaTFA}}$ on the CSS and OSS potential energy surface. (c) The frontier orbitals of $\mathbf{CP1}_{\mathbf{NaTFA}}$ optimized at CASSCF(12,12)/def2-TZVPP level.

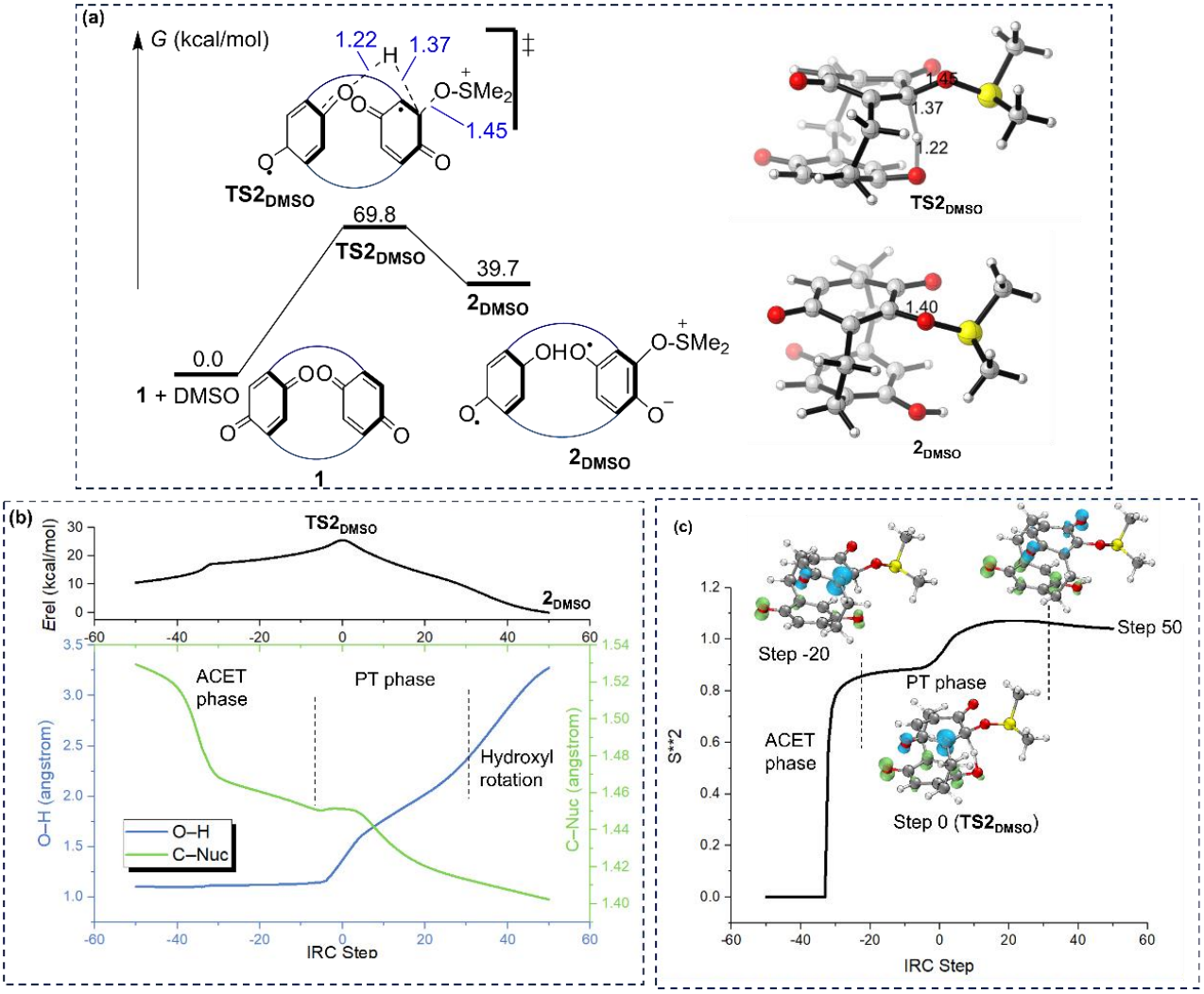

Figure 5. (a) The Gibbs free energy profile for the ACPCET reaction with DMSO as the nucleophile. (b) The evolution of key bond lengths along the IRC of $\mathbf{TS2}_{\mathbf{DMSO}}$ (DMSO). (c) The *S***2 along the IRC, and spin density isosurface of selected points

Quasiclassical Molecular Dynamics Simulation (QCMD). We next turned our attention toward molecular dynamics to gain a more insightful information about the current process. To further study the coupling among each step in real reaction, quasi-classical molecular dynamics trajectories were initiated from **TS2,** and the evolution of key bond lengths was recorded. For all the three nucleophiles, recrossing is quite common, as seen by the nearly doubled number of the trajectories leading to **2** over to **Int2** or separated **1** and nucleophile. The PT event happens rapidly in ~40 fs, regardless of the nucleophile. However, the fate of the trajectories toward the direction of **Int2** (or **Int2'**) is relevant to the nucleophile. In one hand, in the case of NaOMe 5 out of the 14 trajectories lead to close-shelled **Int2**, which is stable during the time period of 300 fs. The evolution of *S***2 for each point (Figure 7e) suggested that the complex returned to be close-shelled in almost ~50 fs, and then the system oscillates between $\mathbf{Int2}_{\mathbf{NaOMe}}$ (*S***2 = 0) and $\mathbf{Int2'}_{\mathbf{NaOMe}}$ (*S***2 ~ 0.8, appears near ~150 fs). On the other hand, in the case of weaker nucleophiles like NaTFA and DMSO, our QCMD results showed a disappearance of $\mathbf{Int2}_{\mathbf{NaTFA}}$ (or $\mathbf{Int2}_{\mathbf{DMSO}}$) and $\mathbf{Int2'}_{\mathbf{NaTFA}}$ (or $\mathbf{Int2'}_{\mathbf{DMSO}}$) with an adequate stability in the trajectories, in which all the trajectories running toward their direction lead to dissociated reactants **1** and nucleophile in a similar timing of ~120 fs. As a result, although the addition reaction with NaTFA and DMSO follows the ACET-PT and ACPCET mechanistic pattern, respectively, they dynamically behave similarly. Both $\mathbf{Int2'}_{\mathbf{NaTFA}}$ or $\mathbf{Int2'}_{\mathbf{DMSO}}$ are not a "dynamically stable" intermediates, and even the ACET and PT steps are sterpwise according to the PES study (Figure 4) in the NaTFA case, the ACET and PT events are dynamically concerted. Finally, these MD simulation results concluded that the coupling between the A, ET and PT reactions might be even stronger in terms of real molecular dynamics behavior than what is expected through a PES-based point of view. An ACET-PT reaction can be dynamically concerted, as shown in the NaTFA case.

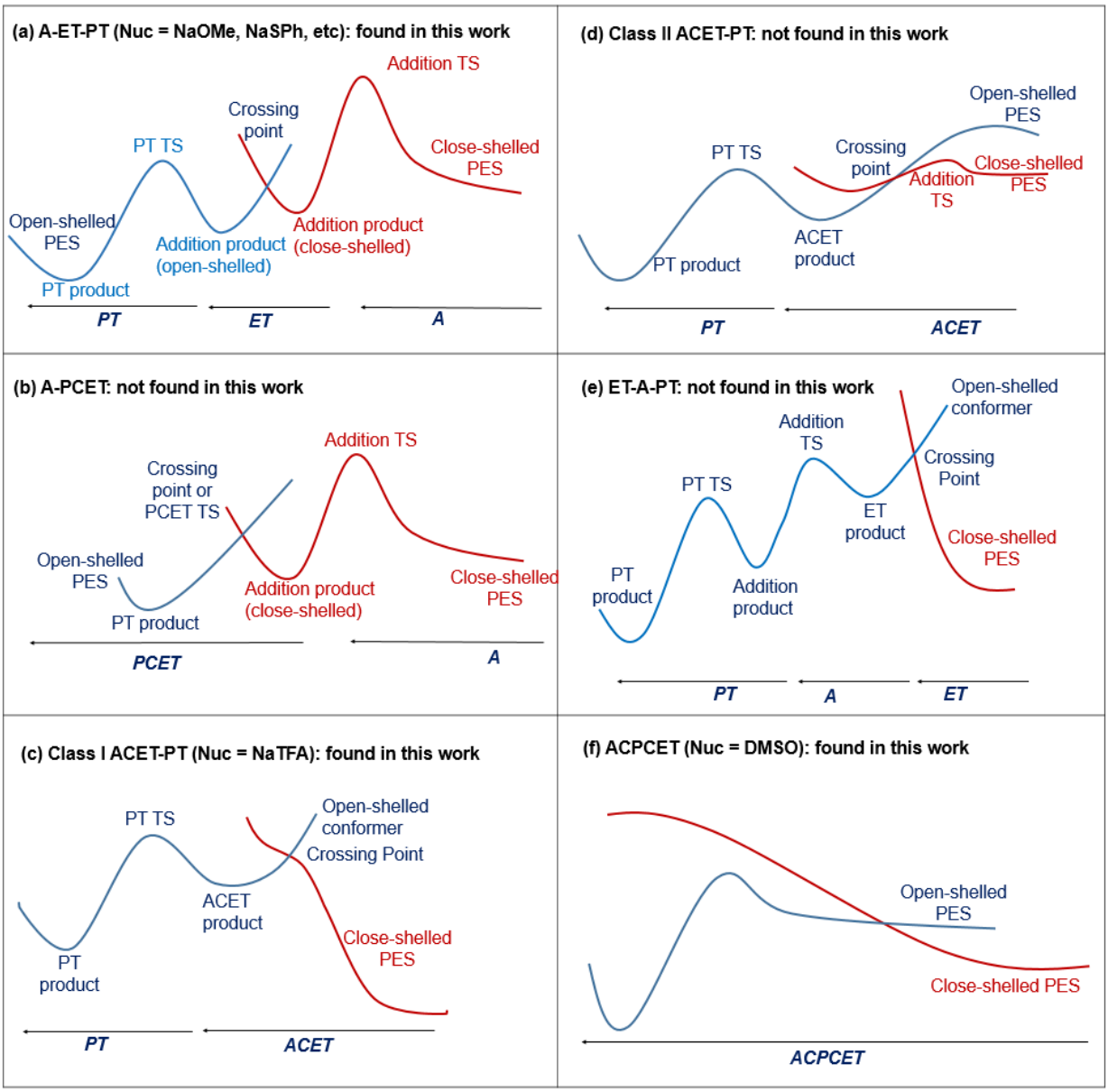

Figure 6. The schematic potential energy surface (PES) for the possible coupling modes among the A, ET, PT reactions.

Conclusion

According to the discussions above, based on DFT and multireference calculations, IRC analysis and quasiclassical molecular dynamics, we have suggested the reaction mode of ACET and ACPCET, in which the addition, proton transfer and electron transfer steps effectively couple in one elementary step. With the [2.2]paracyclophane-derived biquinone **1** as the model substrate, we have shown that the mechanism of nucleophilic addition onto its sp^2 carbon exhibits a consecutive change from stepwise A-ET-PT to ACET-PT and finally to ACPCET. The coupling of A with ET and PT is in consistence with the order of nucleophilicity: when the nucleophile is strong, a stepwise A-ET-PT occurs; otherwise, with an adequately weak nucleophile, the ACET-PT, ACPCET, or other coupling modes has to occur to compensate the unfavorable addition, and which of them occurs depends on the shape of potential energy surface, as shown in Figure 6. Besides, QCMD trajectories show that these steps can be dynamically concerted, even when they seem to be stepwise according to the potential energy surface.

Although the examples of ACET and ACPCET in this work are of extremely high barrier, we believe that there exist other systems that ACET and ACPCET process is able to occur under experimentally accessible condition. For example, before submitting this work, we saw Fujii's latest report[17] on the electron-coupled epoxidation reaction of olefin, with should be another example of ACET. Also, we believe that the remaining three types of coupling not discussed in this work, namely Class II ACET, A-PCET and ET-A-PT, can also be found in the future.[18]

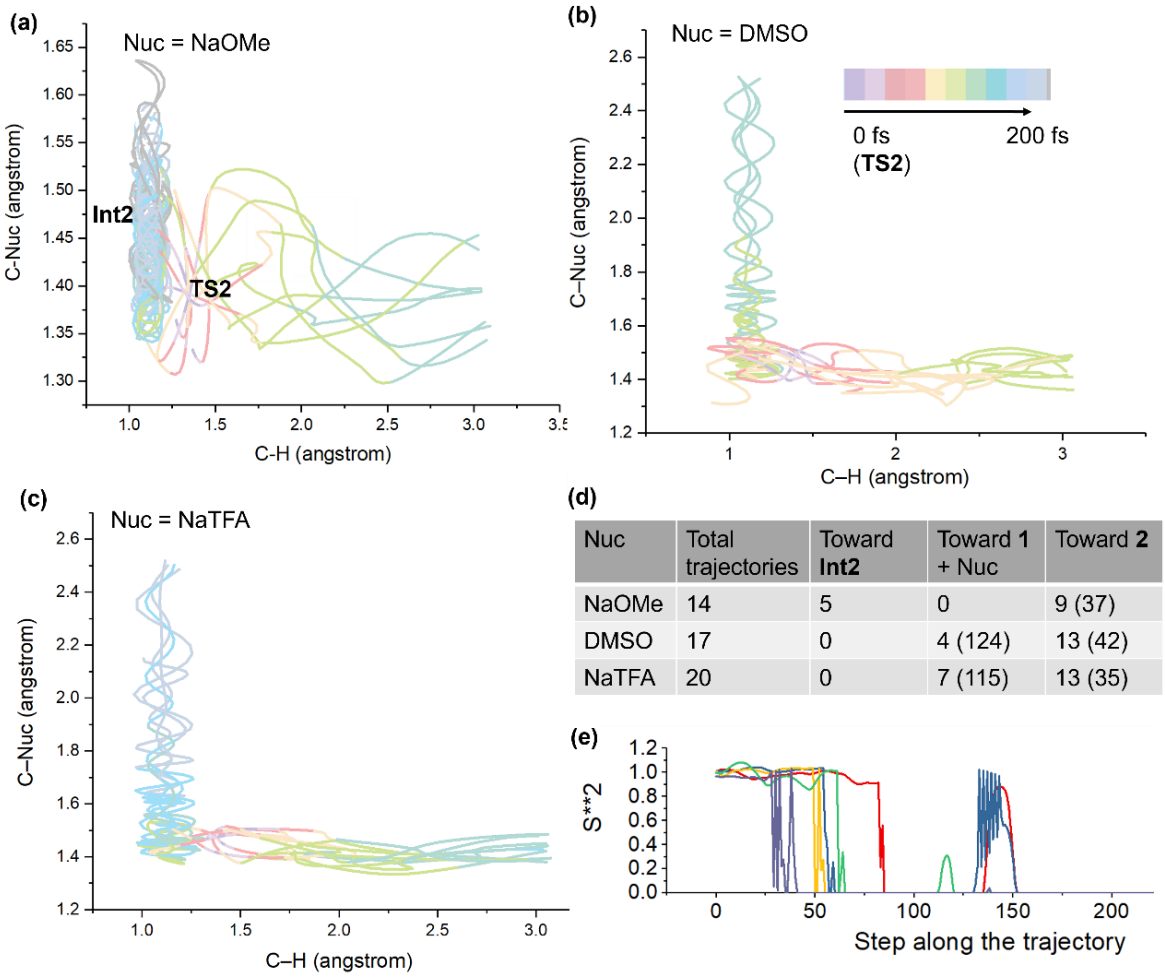

Nuc	Total trajectories	Toward **Int2**	Toward **1** + Nuc	Toward **2**
NaOMe	14	5	0	9 (37)
DMSO	17	0	4 (124)	13 (42)
NaTFA	20	0	7 (115)	13 (35)

Figure 7. (a-c) The evolution of interested bond lengths along the trajectories initiated from **TS2** with various nucleophiles. (d) The numbers of trajectories leading to each outcome. The average timing (fs) is shown in parenthesis. (e) The *S***2 along the trajectories leading to **Int2** (NaOMe) from **TS2** (NaOMe).

As it has been well-known that a weak proton donor or acceptor can be activated by an ET event in a PCET reaction, we expect that the discovery of ACET could shed light on the activation of weak nucleophile or unactivated alkenes. In this work, for example, we have found that the addition product for the extremely weak nucleophile, NaTFA or DMSO, cannot exist as a minimum in the absence of intramolecular oxidant. Similarly, by proper design of ACET systems, we expect that the activation of these weak nucleophiles in a real experimentally accessible condition can be achievable in the future. We also suggest that some of the well-known and of fundamentally important addition reactions in a redox active environment follow ACET mechanism, and our further researches are ongoing.

Acknowledgements

Both authors acknowledged the computational resources provided by Hangzhou Yanqu Information Technology Co., Ltd. Besides, Ma wants to mention a friend Zongchang Han (Tsinghua University); although he does not contribute in this work, he happened to have the concept of ACET in his independent project in 2018, although ACET did not occur in his project. In other words, Han has the idea of ACET earlier than Ma.

References

[1] R. A. Binstead, B. A. Moyer, G. J. Samuels, T. J. Meyer, *J. Am. Chem. Soc.* **1981**, *103*, 2897-2899.

[2] a) M. H. V. Huynh, T. J. Meyer, *Chem. Rev.* **2007**, *107*, 5004-5064; b) J. M. Mayer, *Annu. Rev. Phys. Chem.* **2004**, *55*, 363-390; c) A. Migliore, N. F. Polizzi, M. J. Therien, D. N. Beratan, *Chem. Rev.* **2014**, *114*, 3381-3465; d) R. Tyburski, T. Liu, S. D. Glover, L. Hammarström, *J. Am. Chem. Soc.* **2021**, *143*, 560-576; e) J. J. Warren, T. A. Tronic, J. M. Mayer, *Chem. Rev.* **2010**, *110*, 6961-7001; f) D. R. Weinberg, C. J. Gagliardi, J. F. Hull, C. F. Murphy, C. A. Kent, B. C. Westlake, A. Paul, D. H. Ess, D. G. McCafferty, T. J. Meyer, *Chem. Rev.* **2012**, *112*, 4016-4093; g) S. Hammes-Schiffer, *Acc. Chem. Res.* **2001**, *34*, 273-281; h) S. Hammes-Schiffer, A. A. Stuchebrukhov, *Chem. Rev.* **2010**, *110*, 6939-6960.

[3] a) Q. J. Bruch, G. P. Connor, C.-H. Chen, P. L. Holland, J. M. Mayer, F. Hasanayn, A. J. Miller, *J. Am. Chem. Soc.* **2019**, *141*, 20198-20208; b) E. C. Gentry, R. R. Knowles, *Acc. Chem. Res.* **2016**, *49*, 1546-1556; c) L. Huang, T. Ji, M. Rueping, *J. Am. Chem. Soc.* **2020**, *142*, 3532-3539; d) D. Lehnherr, Y.-h. Lam, M. C. Nicastri, J. Liu, J. A. Newman, E. L. Regalado, D. A. DiRocco, T. Rovis, *J. Am. Chem. Soc.* **2019**, *142*, 468-478; e) S. J. Mora, E. Odella, G. F. Moore, D. Gust, T. A. Moore, A. L. Moore, *Acc. Chem. Res.* **2018**, *51*, 445-453; f) C. B. Roos, J. Demaerel, D. E. Graff, R. R. Knowles, *J. Am. Chem. Soc.* **2020**, *142*, 5974-5979; g) K. Zhao, K. Yamashita, J. E. Carpenter, T. C. Sherwood, W. R. Ewing, P. T. Cheng, R. R. Knowles, *J. Am. Chem. Soc.* **2019**, *141*, 8752-8757.

[4] Y. Ma, A. Hussein, *ChemRxiv* **2021**, DOI: 10.26434/chemrxiv-2021-qlh3r-v4.

[5] M. J. Frisch, G. W. Trucks, H. B. Schlegel, G. E. Scuseria, M. A. Robb, J. R. Cheeseman, G. Scalmani, V. Barone, G. A. Petersson, H. Nakatsuji, X. Li, M. Caricato, A. V. Marenich, J. Bloino, B. G. Janesko, R. Gomperts, B. Mennucci, H. P. Hratchian, J. V. Ortiz, A. F. Izmaylov, J. L. Sonnenberg, Williams, F. Ding, F. Lipparini, F. Egidi, J. Goings, B. Peng, A. Petrone, T. Henderson, D. Ranasinghe, V. G. Zakrzewski, J. Gao, N. Rega, G. Zheng, W. Liang, M. Hada, M. Ehara, K. Toyota, R. Fukuda, J. Hasegawa, M. Ishida, T. Nakajima, Y. Honda, O. Kitao, H. Nakai, T. Vreven, K. Throssell, J. A. Montgomery Jr., J. E. Peralta, F. Ogliaro, M. J. Bearpark, J. J. Heyd, E. N. Brothers, K. N. Kudin, V. N. Staroverov, T. A. Keith, R. Kobayashi, J. Normand, K. Raghavachari, A. P. Rendell, J. C. Burant, S. S. Iyengar, J. Tomasi, M. Cossi, J. M. Millam, M. Klene, C. Adamo, R. Cammi, J. W. Ochterski, R. L. Martin, K. Morokuma, O. Farkas, J. B. Foresman, D. J. Fox, Wallingford, CT, **2016**.

[6] J.-D. Chai, M. Head-Gordon, *Phys. Chem. Chem. Phys.* **2008**, *10*, 6615-6620.

[7] F. Weigend, R. Ahlrichs, *Phys. Chem. Chem. Phys.* **2005**, *7*, 3297-3305.

[8] A. V. Marenich, C. J. Cramer, D. G. Truhlar, *J. Phys. Chem. B* **2009**, *113*, 6378-6396.

[9] T. Lu, F. Chen, *J. Comput. Chem.* **2012**, *33*, 580-592.

[10] C. Legault, *Université de Sherbrooke* **2009**.

[11] W. Humphrey, A. Dalke, K. Schulten, *J. Mol. Graph.* **1996**, *14*, 33-38.

[12] D. A. Singleton, C. Hang, M. J. Szymanski, E. E. Greenwald, *J. Am. Chem. Soc.* **2003**, *125*, 1176-1177.

[13] C. Angeli, R. Cimiraglia, S. Evangelisti, T. Leininger, J.-P. Malrieu, *J. Chem. Phys.* **2001**, *114*, 10252-10264.

[14] a) F. Neese, *Wiley Interdisciplinary Reviews: Computational Molecular Science* **2018**, *8*, e1327; b) F. Neese, F. Wennmohs, U. Becker, C. Riplinger, *J. Chem. Phys.* **2020**, *152*, 224108.

[15] Y. Ma,. **2022**. https://github.com/RimoAccelerator/KST48.

[16] W. Rebafka, H. A. Staab, *Angew. Chem.* **1973**, *85*, 831-832.

[17] Y. Ishimizu, Z. Ma, M. Hada, H. Fujii, *Inorg. Chem.* **2021**, *60*, 17687-17698.

[18] As another example, we have examined the role of ACET in formal Diels-Alder reaction: Y. Ma, *ChemRxiv* **2022**, DOI:10.26434/chemrxiv-2022-zt155-v2.